

## The Usefulness of Density Functional Theory To Describe the Tautomeric Equilibrium of 4,6-Dimethyl-2-mercaptopyrimidine in Solution

Raul Martos-Calvente, Victor. A. de la Peña O'Shea, Jose M. Campos-Martin, and Jose L. G. Fierro\*

*Instituto de Catálisis y Petroleoquímica, CSIC, Cantoblanco, 28049 Madrid, Spain*

*Received: March 18, 2003; In Final Form: May 13, 2003*

The tautomeric forms of 4,6-dimethyl-2-mercaptopyrimidine in solution were examined. Experimental support for the existence of the tautomeric forms of this molecule was provided by infrared (FTIR), ultraviolet (UV), and nuclear magnetic resonance (NMR) techniques. Density functional theory (DFT) calculations allowed us to elucidate these molecular structures. The vibrational and electronic spectra, as well as the  $^1\text{H}$  and  $^{13}\text{C}$  chemical shifts, were satisfactorily described by DFT theoretical calculations. The potential of the DFT methodology was confirmed by prediction of a band at  $2706\text{ cm}^{-1}$ , associated with the stretching vibration of  $-\text{SH}$  group, which did not appear in the experimental spectrum because it was overshadowed by the symmetric and antisymmetric vibration modes of  $-\text{CH}_3$  groups. The existence of the tautomeric thiol–thione equilibrium of 4,6-dimethyl-2-mercaptopyrimidine with the thione structure dominating in polar solvents ( $\text{CH}_3\text{OH}$  and  $\text{DMSO}-d_6$ ) and the thiol structure in apolar media (cyclohexane) has been demonstrated.

### Introduction

Owing to their many fields of application, mercaptopyrimidines have been widely studied over the past few years.<sup>1</sup> The chemistry of mercaptopyrimidines that incorporate both S and N atoms in their structure is rich because these compounds can coordinate as monodentate ligands<sup>2</sup> and more frequently as polydentate ligands either to a single metal center, acting as a chelating ligand,<sup>3,4</sup> or to several metal centers as a bridging ligand.<sup>5</sup> These compounds exhibit tautomeric equilibrium between the thiol ( $>\text{C}-\text{SH}$ ) and thione ( $>\text{C}=\text{S}$ ) as a consequence of the highly mobile protons that they possess (Figure 1).<sup>6–9</sup> The predominant form largely depends on the state and conditions of the molecule. Thus, from X-ray diffraction, it has been demonstrated that 2-mercaptopyrimidine exhibits a predominant thione form in the solid state, although it can also develop dimeric structures through hydrogen bridges.<sup>9–11</sup> However, in liquid phase, there are several additional factors involved in the shift of tautomeric equilibrium. Among these, the solvent, temperature, pH, and concentration remain prominent.<sup>12</sup> Thus, it has been demonstrated by means of UV spectroscopy that the thione predominates over the thiol form and dimer formation can be shifted toward the thiol form by increasing the temperature or by decreasing the concentration in an apolar solvent.<sup>8</sup> NMR studies also provide evidence concerning the predominance of the thione structure; inclusively, the prototropic interconversion between the tautomers has been reported.<sup>13</sup> Infrared is another valuable instrument to investigate the chemical structure of these compounds and derivatives and has allowed several experiments to be performed the results of which allow full interpretation of their vibrational spectra.<sup>14,15</sup>

These compounds belong to a class of reagents that are very useful in organic synthesis because they offer the possibility of investigating alternative routes to conventional processes,

specifically that involving nucleophilic substitutions.<sup>16</sup> However, their full potential is beyond the scope of this article because they have found numerous applications in organometallic chemistry.<sup>1,2,5,17–19</sup> The principal interest in these organometallic complexes is not only from the descriptive but also from the practical point of view because they have been used in quite varied applications such as in biochemistry, medicine, or catalysis. Thus, zinc and tin complexes have been described as polyolefin stabilizers. Zinc 2-mercaptopyrimidine oxide has bacteriostatic, antifungal, and antiseborrheic properties,<sup>20</sup> and the Pt–2-mercaptopyrimidine complex exhibits antitumoral activity.<sup>21</sup> Quite different applications are found in the field of catalysis, and particularly attractive in this sense are the epoxidation of primary alkenes with molybdenum complexes containing 4,6-dimethyl-2-mercaptopyrimidine<sup>22</sup> or hydroformylation reactions with rhodium or iridium complexes.<sup>23,24</sup> In all of these structures, the nature of the resulting coordination compounds appears to be influenced by the tautomeric form of the ligand molecules that result in the formation of chelated compounds with a coordination of 4, 5, or 6.<sup>18,19</sup>

In light of the preceding, the present work was undertaken with the aim of studying the tautomeric forms of the 4,6-dimethyl-2-mercaptopyrimidine compound as a previous step to understanding the structure of its complexes with transition metals. Experimental support for the existence of the tautomeric forms of this molecule was gained from infrared (FTIR), ultraviolet (UV), and nuclear magnetic resonance (NMR) techniques. Further insight into the molecular structures was provided by theoretical calculations using the density functional theory (DFT) approach.

### Experimental Section

FTIR spectra were recorded with a resolution of  $4\text{ cm}^{-1}$  on a Nicolet 510 FT-IR spectrophotometer, using KBr wafers containing 1% of the sample. NMR spectra were acquired with a Bruker DRX-500 equipment, and the samples were dissolved in  $\text{DMSO}-d_6$ . UV–vis spectra were obtained on a Shimadzu

\* To whom correspondence should be addressed. Fax: +34 915854760. E-mail address: jlgfierro@icp.csic.es. Web address: <http://www.icp.csic.es/eac/index.htm>.

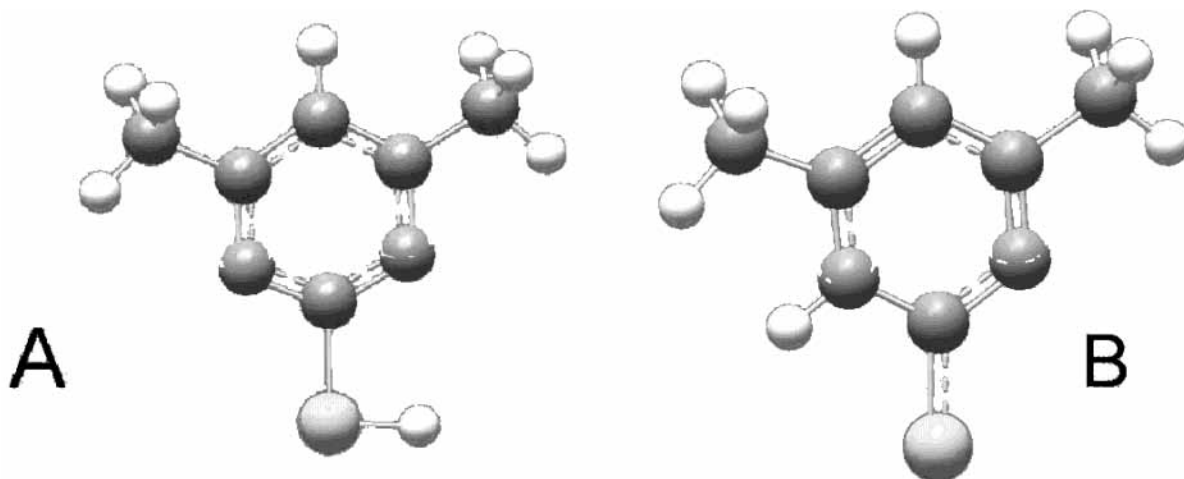


**Figure 1.** Optimized geometry of the tautomeric species of 4,6-dimethyl-2-mercaptopyrimidine: (a) thiol; (b) thione.

UV 2100 spectrophotometer, using methanol and cyclohexane solutions containing 1% of the samples.

**Computational Methods.** Calculations were performed with the Gaussian 98, A.10 version, suite of programs.<sup>25</sup> Full geometry optimizations of the thiol and thione structures (Figure 1) were performed using Berny's optimization algorithm (calculating the energy derivatives with respect to nuclear coordinates analytically).<sup>26</sup> In both cases, the gradient-corrected density functional methodology was employed: Becke's exchange functional (B3)<sup>27</sup> and Becke's three-parameter adiabatic connection (B3) hybrid<sup>28</sup> exchange functional were used in combination with the Lee–Yang–Parr correlation functional.<sup>29</sup> In all cases, the standard 6-31G\*\* basis set of DZP quality was used for orbital expansion to solve the Kohn–Sham equations. Subsequently, the harmonic vibrational frequencies and IR intensities were calculated at the same level of theory. To avoid systemic errors in calculated frequencies, computed frequencies have been scaled.<sup>30</sup>

<sup>1</sup>H and <sup>13</sup>C magnetic shielding tensors ( $\chi$ ) of DFT-optimized structures of 9-acridinones, and TMS as reference, were obtained following the gauge-including atomic orbital (GIAO) approach at the DFT level.<sup>31–33</sup> To compare isotropic shieldings with the experimentally observed chemical shifts, the NMR parameters for TMS (tetramethylsilane) were calculated and used as the reference molecule.

Photophysical properties were calculated using time-dependent density functional theory (TD-DFT)<sup>34</sup> with 6-31G\*\* basis set. TD-DFT generalizes density functional theory to a time-dependent situation in which a system is subjected to a time-dependent perturbation, which modifies its external potential. In Kohn–Sham formalism, time-dependent Kohn–Sham equations can be derived by assuming the existence of an effective potential for an independent particle model of which the orbital gives the same density as that of the interacting system. In response theory, transition energies and oscillator strengths can be determined from the response of the charge density to a perturbation.

## Results and Discussion

The energy of the two tautomers in an apolar (cyclohexane) and another polar (methanol) solvent was calculated by DFT. While the energy calculations for gas-phase species indicated that the thiol structure is the most stable species ( $\Delta E = 7.9$  kJ/mol), energy values became very close to each other ( $\Delta E < 0.25$  kJ/mol) once a solvent such as cyclohexane was included

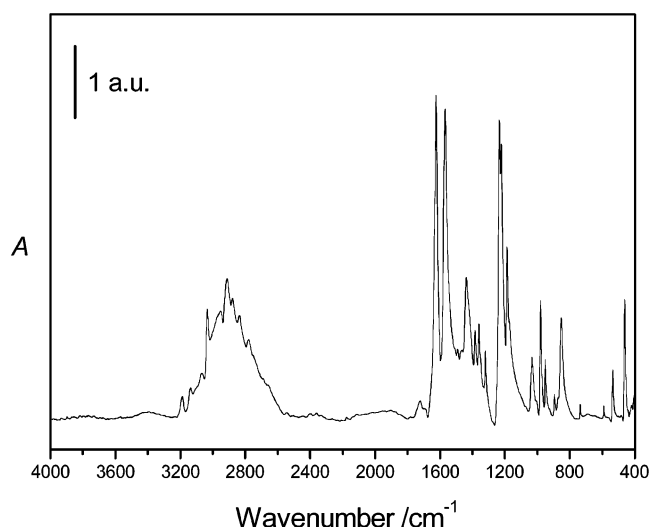


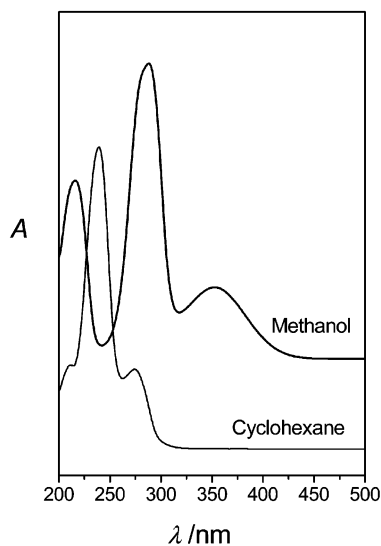
**Figure 2.** Experimental FTIR spectrum of the solid 4,6-dimethyl-2-mercaptopyrimidine sample.

in calculations. This result points to the coexistence of the two species of the tautomeric equilibrium. Indeed, it was clearly stated that the thione structure is much more stable ( $\Delta E = 23.8$  kJ/mol) in a polar medium, which agrees with literature findings.<sup>8,9</sup>

The infrared spectrum of a 4,6-dimethyl-2-mercaptopyrimidine sample diluted in potassium bromide revealed the characteristic vibration bands of this compound (Figure 2). The assignments of the different bands of this compound are shown in Table 1. A broad band at  $3450\text{ cm}^{-1}$  could be attributed to  $\nu(\text{N-H})$  interacting with residual water in the IR wafer. The bands at  $3185$  and  $3140\text{ cm}^{-1}$  belong to  $\nu(\text{C-H})$  vibration.<sup>35</sup> The band at  $461\text{ cm}^{-1}$  is attributed to  $\nu(\text{C=S})$  and  $\beta(\text{C=S})$  vibrations.<sup>35</sup> Because intermolecular interactions are expected to occur, it is likely that hydrogen bridges will be developed. Thus, the band at  $2835\text{ cm}^{-1}$  should be attributed to the  $\nu(\text{NH}\cdots\text{S})$  interaction.<sup>36</sup> A weak band observed at  $1728\text{ cm}^{-1}$  could be responsible for the SCN group.<sup>14</sup> The vibration of the  $\text{NHC=S}$  group shows peaks at  $1225$  and  $1188\text{ cm}^{-1}$ .<sup>16</sup> The bands at  $1624$  and  $1565\text{ cm}^{-1}$  are assigned to  $\nu(\text{C=C}) + \nu(\text{C=N})$  vibrations.<sup>16</sup> Finally, the  $\nu(\text{N=C})$  vibration gives rise to a band at  $1437\text{ cm}^{-1}$ , which also contains the  $\delta(\text{CH}) + \delta(\text{NH})$  deformation.<sup>21</sup> It should be stressed that all of the above bands are typical of the thione structure and in no case could bands of the thiol group be discerned. In any case, if present, they

**TABLE 1: Assignment of IR Bands of Solid Sample**

vibration	exptl band, $\text{cm}^{-1}$	thione (DFT), $\text{cm}^{-1}$	thiol (DFT), $\text{cm}^{-1}$
$\nu(\text{N-H})$	3450 w	3582	
$\nu(\text{C-H})_{\text{asym}}$	3185m, 3140m	3115, 3142	3107, 3163
$\nu(\text{C-H})_{\text{sym}}$	3030–2920s	3056, 3070	3049
	several bands		
$\nu(\text{NH}\cdots\text{S})$	2835m		
SCN group	1728w	1684	
$\nu(\text{C}=\text{C}) + \nu(\text{C}=\text{N})$	1624vs, 1565vs	1637, 1541	1624, 1598
$\nu(\text{N}=\text{C}) + \delta(\text{CH}) + \delta(\text{NH})$	1437s	1472	1445
$\text{CH}_3$ sym def	1380m, 1360m	1372	1378
$\nu(\text{C}=\text{S})$ in $\text{NHC}=\text{S}$	1225vs, 1188s	1226, 1173	1304, 1297
$\text{CH}_3$ rocking	1032m, 952m	1096	1029
ring stretching, $\beta(\text{N-H})$	980s	970	
$\gamma(\text{N-H})$	850s	828	
$\nu(\text{C}=\text{S}), \beta(\text{C}=\text{S})$	461s	482	

**Figure 3.** UV–vis spectra of 4,6-dimethyl-2-mercaptopyrimidine in different solvents.

would be overshadowed by those of the thione. The rest of the bands (Table 1) are associated with methyl groups and aromatic ring vibrations. Thus, the infrared spectra provide experimental evidence that thione is the dominant species in the solid state, in agreement with earlier reports in the literature.<sup>8,9,14</sup>

DFT calculations aimed at describing the vibrational structure of the two tautomeric species point to good agreement with the experimental infrared spectra, as shown in Table 1. The wavenumbers of the characteristic infrared bands described above fit those predicted by the theoretical model fairly well. Additionally, the DFT calculations provide some interesting clues that initially could not be gained from inspection of the experimental infrared spectra. An example illustrating the potential of the DFT calculations is the prediction of a band at  $2706 \text{ cm}^{-1}$  attributed to the stretching vibration of  $-\text{SH}$  group that did not appear in the experimental spectra because it was overshadowed by the symmetric and antisymmetric vibration modes of  $-\text{CH}_3$  groups.

UV–vis spectra of the sample dissolved in methanol and in cyclohexane are compared in Figure 3. The electronic spectra of the sample in methanol exhibited three bands at 217, 289, and 355 nm and changed substantially when cyclohexane was used. In the latter case, a major band at 238 nm and two weaker ones at 213 and 275 nm were clearly distinguished. As documented in the literature and in agreement with the DFT calculations, bands at 215, 280, and 355 nm correspond to the

**TABLE 2: Experimental and DFT-Calculated UV–vis Spectra of the Sample**

exptl band, nm		DFT, nm	
methanol	cyclohexane	thione	thiol
216	213	201	
288	275	267	
354		378	
	238		233

**TABLE 3: Experimental and DFT-Calculated  $^1\text{H}$  NMR Spectra of the Sample in DMSO Solvent**

atom	signal	chemical shift $\delta$ , ppm	intensity	chemical shift $\delta$ (DFT), ppm	
				thione	thiol
$\text{H}_a$	S	13.45	0.15	8.49	
$\text{H}_b=\text{H}_c$	S	2.20	12.50	2.1	
$\text{H}_d$	S	6.52	3.36	5.68	
$\text{H}_e=\text{H}_g$	S	2.25	1.28		2.1
$\text{H}_h$	S	6.94	0.18		6.47

thione form (Table 2),<sup>8</sup> while that at 238 nm is attributed to the thiol form (Table 2).<sup>8</sup> These observations demonstrate that the tautomeric thione structure is favored in polar solvents, while the thiol structure dominates in apolar media.<sup>9</sup>

TD-DFT calculations aimed at studying the electronic structure and possible UV–vis transitions of the tautomer provided additional support for the stability of both molecules in different solvents. For this purpose, the stability of each tautomer was examined in the solvents methanol (polar) and cyclohexane (apolar) with a view to investigating the effect of polarity on the equilibrium of both tautomers in liquid phase. The DFT calculations again indicated good agreement with the experimentally detected wavelengths of the electronic transitions of 4,6-dimethyl-2-mercaptopyrimidine in these two solvents (Table 2). The characteristic electronic transitions of each of the tautomers show that the thione structure dominates in polar solvents while the thiol form is the major species in apolar solvents. The orbitals involved in these transitions are depicted in Figures 4 and 5. In the case of thiol, only a single band corresponding to a  $\pi \rightarrow \pi^*$  type transition is present, HOMO and LUMO+1 being the only orbitals involved in such a transition. In the case of the thione, the three bands corresponding to a  $\pi \rightarrow \pi^*$  type transition are observed, the most intense thione band involving HOMO-1, and LUMO, and LUMO+1. We did not observe differences in the calculated energy of the characteristic electronic transitions of each tautomer using different solvents (methanol or cyclohexane); thus, the experimental observation of the change in the UV–vis spectrum should be due to a change in the population of the thiol and thione forms.

The  $^1\text{H}$  NMR spectra of 4,6-dimethyl-2-mercaptopyrimidine in  $\text{DMSO}-d_6$  are shown in Table 3. To facilitate band identification, the atoms are clearly labeled in Figure 6. The sample in liquid  $\text{DMSO}-d_6$  exhibited a broad band at  $\delta = 13.45$  ppm, characteristic of  $\text{N-H}$  bonds, while that of  $\text{S-H}$  was broad and weak due to the low proportion of the thiol form and hence cannot be discerned. However, proton signals in the para position at 6.95 ppm for the thiol form and at 6.52 ppm for the thione form, the latter being much more intense, can be appreciated. The  $^1\text{H}$  signal of the methyl groups depends on each of the tautomeric forms. Thus, characteristic features at +2.25 and +2.20 ppm, the latter more intense than the former, are observed for the thiol and thione structures, respectively. These data provide additional support that the thione form dominates in the polar solvent.<sup>13</sup> A rough estimation of the proportion of the



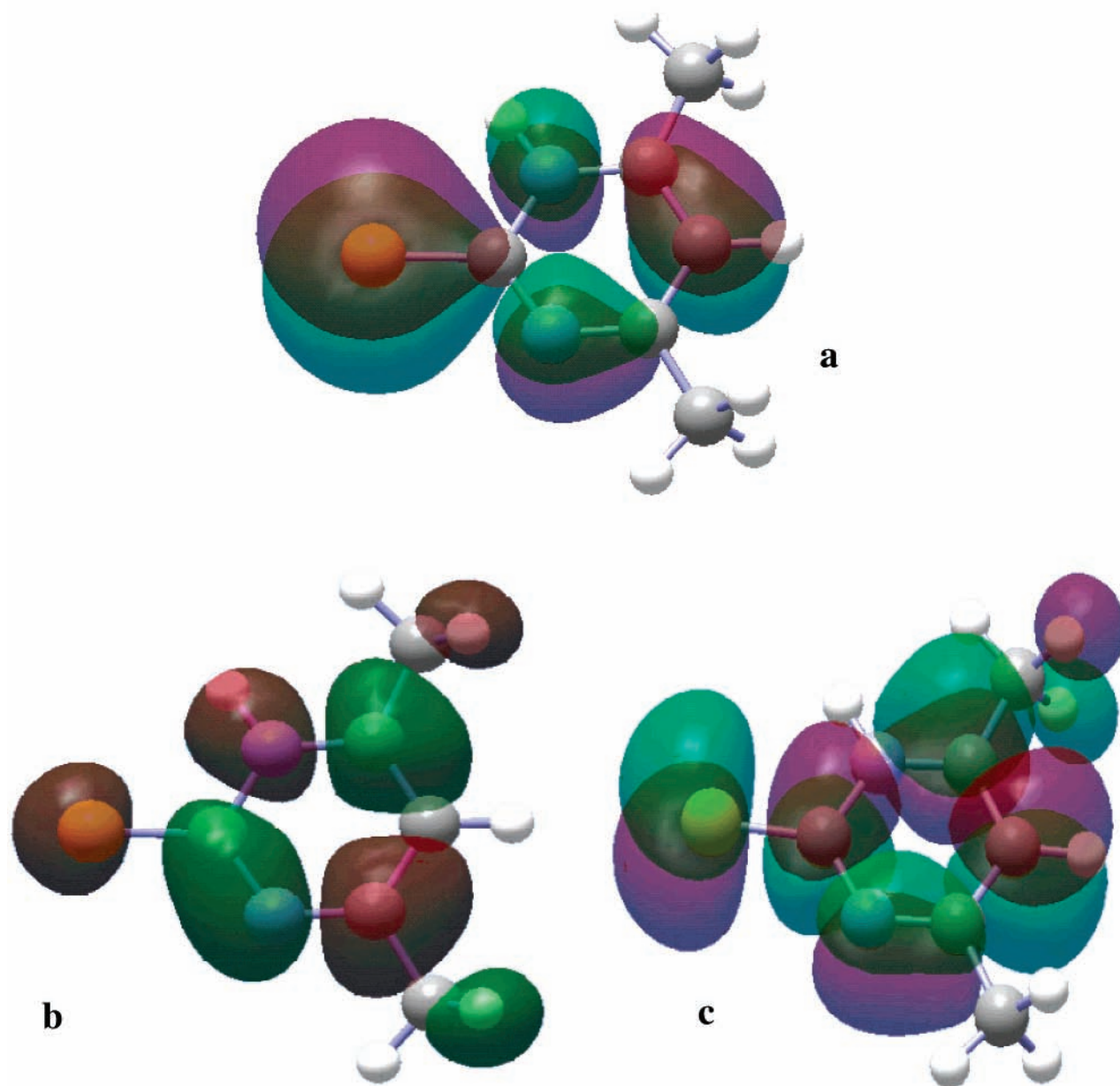


**Figure 4.** Molecular orbitals involved in the electronic transitions for the thione tautomer: (a) HOMO-1; (b) LUMO; (c) LUMO+1.

**TABLE 4: Experimental and DFT-Calculated  $^{13}\text{C}$  NMR Spectra of the Sample in DMSO Solvent**

atom	chemical shift $\delta$ , ppm	intensity	chemical shift $\delta$ (DFT), ppm	
			thione	thiol
C(1)	181.77	12.50	178.2	
C(2)	159.37	0.10	151.8	
C(4)	110.62	6.24	97.45	
C(1')	168.51	0.99		170.4
C(2')	162.51	0.08		158.2
C(4')	118.49	0.20		107.2

two tautomers was obtained by integrating the experimental proton signals, showing 95% for the thione and only 5% for the thiol form.

$^{13}\text{C}$  NMR spectra also provided valuable information concerning the nature and abundance of each tautomer in solution. The  $^{13}\text{C}$  NMR spectra of 4,6-dimethyl-2-mercaptopyrimidine in DMSO- $d_6$  are shown in Table 4. A peak characterized by its chemical shift at  $\delta = +181.77$  ppm arising from carbon atom C(1) is much intense than that of carbon atom C(1') of the thiol

structure. A similar trend is observed for the signals of carbon atoms C(4) and C(4'). Unfortunately, the carbon atoms of the methyl groups are not well resolved, and only a broad component at  $\delta = +22$  ppm can be discerned. These observations agree with the information drawn from the  $^1\text{H}$  NMR spectra and confirm the existence of tautomeric thiol–thione equilibrium with the thione structure dominating in polar solvents.<sup>13</sup>

Tables 3 and 4 summarize the experimental and DFT-simulated NMR spectra of the two tautomer forms of the 4,6-dimethyl-2-mercaptopyrimidine molecule. Scrutiny of the data offered in these tables clearly reveals that the experimental  $^1\text{H}$  and  $^{13}\text{C}$  chemical shifts are consistent with those calculated theoretically. Some discrepancies are seen, however, in the case of the thione proton  $\text{H}_a$  in which the effect of the solvent is greater. Additional DFT calculations using different solvents are currently in progress in an attempt to explain the observed chemical shifts in the NMR spectra.

It should be noted that the tautomeric thione–thiol equilibrium in N-containing heterocycles has long been investigated

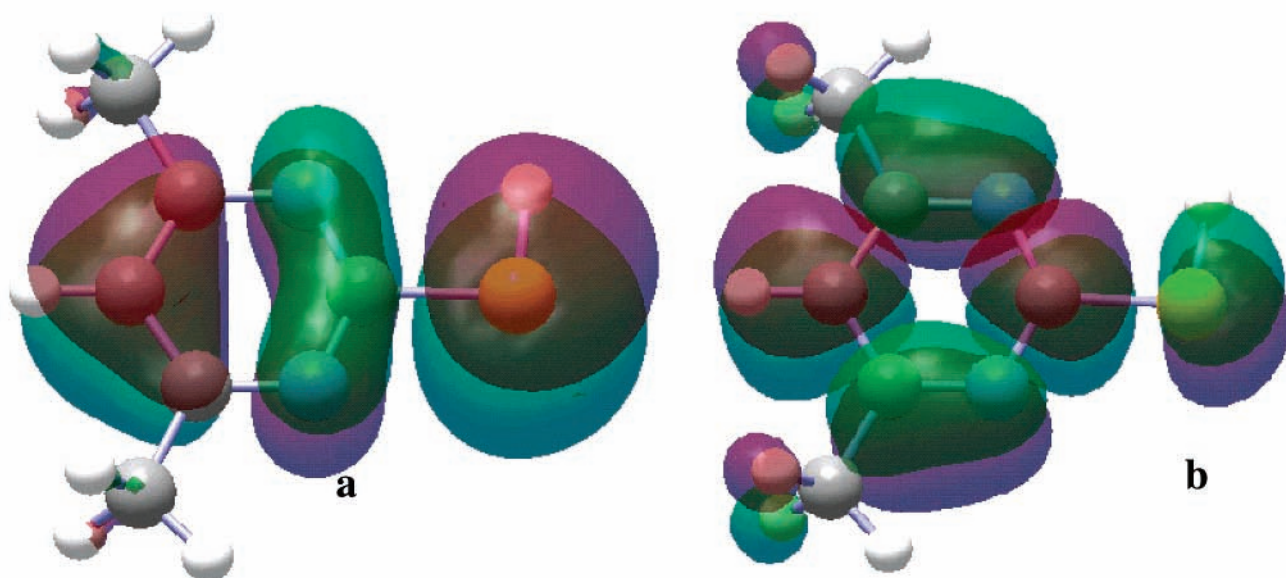


**Figure 5.** Molecular orbitals involved in the electronic transitions for the thiol tautomer: (a) HOMO; (b) LUMO+1.

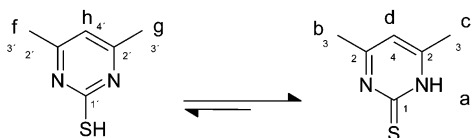


**Figure 6.** Atom nomenclature employed for NMR assignments.

from the experimental point of view;<sup>9</sup> most specifically for the case of 2-mercaptopyrimidine. This knowledge allowed us not only to combine an experimental methodology with the extremely useful contribution of theoretical study provided by DFT methodology but also to investigate the 4,6-dimethyl-2-mercaptopyrimidine molecule itself, for which no previous analysis has been achieved using DFT analysis. From the data compiled in the present study, it is clear that a close similarity exists between the results derived from computational methods (DFT) and those obtained by experimental techniques. This parallelism emphasizes the usefulness of theoretical calculations to predict and describe the experimental observations during the tautomeric equilibrium of 4,6-dimethyl-2-mercaptopyrimidine. Thus, the number and type of signals observed with FTIR, UV-vis, and NMR spectroscopic techniques could be unambiguously assigned. This confirms the potential of advanced computational DFT methods for the identification and characterization of chemical structures along the study with experimental spectroscopic techniques. It has been reliably confirmed that the thione form dominates in the solid state (Table 1), together with the great importance of the polarity of the solvent in shifting the tautomeric equilibrium, thione being the dominant species in polar solvents (methanol and DMSO-*d*<sub>6</sub>) and the thiole structure in apolar media (cyclohexane).

## Conclusions

The tautomeric forms of the 4,6-dimethyl-2-mercaptopyrimidine compound were revealed by infrared (FTIR), ultraviolet (UV), and nuclear magnetic resonance (NMR) techniques. Density functional theory (DFT) calculations allowed us to elucidate these molecular structures. DFT calculations aimed at describing the vibrational structure of the two tautomeric species fit fairly well with the experimental infrared spectra, as shown in Table 1. The potential of the DFT methodology was confirmed by prediction of a band at 2706 cm<sup>-1</sup>, associated

with the stretching vibration of -SH group, which did not appear in the experimental spectrum because it was overshadowed by the symmetric and antisymmetric vibration modes of -CH<sub>3</sub> groups. Similarly, DFT calculations again indicated good agreement with the experimentally detected wavelengths of the electronic transitions in the two solvents, the thione structure dominating in polar solvents (CH<sub>3</sub>OH and DMSO-*d*<sub>6</sub>) and the thiol form in apolar (cyclohexane) medium. In line with the above, the experimental <sup>1</sup>H and <sup>13</sup>C chemical shifts are consistent with those predicted by the theoretical model. Some discrepancies are seen, however, in the case of the thione proton H<sub>a</sub>, in which the effect of the solvent is greater.

**Acknowledgment.** The authors acknowledge financial support from Repsol-YPF (Spain). Two of us (R.M.C. and J.M.C.M.) gratefully acknowledge fellowships also granted by Repsol-YPF.

## References and Notes

- (1) Senge, M. O. *Angew. Chem., Int. Ed. Engl.* **1996**, *35*, 1923.
- (2) Raper, E. S. *Coord. Chem. Rev.* **1996**, *153*, 199.
- (3) Fandos, R.; Lafranchi, A.; Otero, A.; Pellinghelli, M. A.; Ruiz, M. J.; Terreros, P. *Organometallics* **1996**, *15*, 4725.
- (4) Brandt, K.; Sheldrick, W. S. *Inorg. Chim. Acta* **1998**, *267*, 39.
- (5) Raper, E. S. *Coord. Chem. Rev.* **1996**, *165*, 475.
- (6) Spinner, E. *J. Chem. Soc.* **1960**, 1237.
- (7) Jones, R. A.; Katrinzky, A. R. *J. Chem. Soc.* **1958**, 3610.
- (8) Stoyanov, S.; Petrov, I.; Antonov, L.; Stoyanov, T.; Karagiannidis, P.; Aslanidis, P. *Can. J. Chem.* **1990**, *68*, 1482.
- (9) Stoyanov, S.; Stoyanov, T.; Akrivos, P. D. *Trends Appl. Spectrosc.* **1998**, *2*, 89.
- (10) Penfold, B. R. *Acta Crystallogr.* **1953**, *6*, 707.
- (11) Beak, P.; Fry, I. S.; Lee, J.; Steela, F. *J. Am. Chem. Soc.* **1976**, *98*, 171.
- (12) Perrin, D. D. *Dissociation constants of organic bases in aqueous solution*; Butterworths: London, 1956; p 164.
- (13) Kashima, C.; Katoh, A.; Shimizu, M.; Omote, Y. *Heterocycles* **1984**, *22* (11), 2591.
- (14) Gupta, S. P.; Sharma, S.; Goel, R. K. *Spectrochim. Acta* **1986**, *42A* (10), 1171.
- (15) Guo-Sheng, H.; Yong-Hong, L.; Bao-Hua, C.; Yong-Xiang, M. *Chem. Pap.* **1999**, *53* (1), 65.
- (16) Ismail, M. M.; Abass, M.; Hassan, M. *Molecules* **2000**, *5*, 1224.
- (17) Raper, E. S. *Coord. Chem. Rev.* **1994**, *129*, 91.
- (18) Bayon, J. C.; Claver, C.; Masdeu-Bulto, A. M. *Coord. Chem. Rev.* **1999**, *193–195*, 73.
- (19) Akrivos, P. D. *Coord. Chem. Rev.* **2001**, *213*, 181.
- (20) Raper, E. S. *Coord. Chem. Rev.* **1985**, *61*, 115.

- (21) Cervantes, G.; Marchal, S.; Prieto, M. J.; Pérez, J. M.; González, V. M.; Alonso, C.; Moreno, V. *J. Inorg. Biochem.* **1999**, *77* (3–4), 197.
- (22) Martos Calvente, R.; Campos-Martín, J. M.; Fierro, J. L. G. *Catal. Commun.* **2002**, *3*, 247.
- (23) Rojas, S.; Fierro, J. L. G.; Fandos, R.; Rodríguez, A.; Terreros, P. *J. Chem. Soc., Dalton Trans.* **2001**, 2316.
- (24) Rojas, S.; Terreros, P.; Fierro, J. L. G. *J. Mol. Catal. A: Chem.* **2002**, *184*, 19.
- (25) Frisch, M. J.; Trucks, G. W.; Schlegel, H. B.; Scuseria, G. E.; Robb, M. A.; Cheeseman, J. R.; Zakrzewski, V. G.; Montgomery, J. A., Jr.; Stratmann, R. E.; Burant, J. C.; Dapprich, S.; Millam, J. M.; Daniels, A. D.; Kudin, K. N.; Strain, M. C.; Farkas, O.; Tomasi, J.; Barone, V.; Cossi, M.; Cammi, R.; Mennucci, B.; Pomelli, C.; Adamo, C.; Clifford, S.; Ochterski, J.; Petersson, G. A.; Ayala, P. Y.; Cui, Q.; Morokuma, K.; Malick, D. K.; Rabuck, A. D.; Raghavachari, K.; Foresman, J. B.; Cioslowski, J.; Ortiz, J. V.; Stefanov, B. B.; Liu, G.; Liashenko, A.; Piskorz, P.; Komaromi, I.; Gomperts, R.; Martin, R. L.; Fox, D. J.; Keith, T.; Al-Laham, M. A.; Peng, C. Y.; Nanayakkara, A.; Gonzalez, C.; Challacombe, M.; Gill, P. M. W.; Johnson, B. G.; Chen, W.; Wong, M. W.; Andres, J. L.; Head-Gordon, M.; Replogle, E. S.; Pople, J. A. *Gaussian 98*, revision A.10; Gaussian, Inc.: Pittsburgh, PA, 1998.
- (26) Schlegel, H. B. *J. Comput. Chem.* **1982**, *3*, 214.
- (27) Becke, A. D. *Phys. Rev. A* **1988**, *38*, 3098.
- (28) Becke, A. D. *J. Chem. Phys.* **1993**, *98*, 5648.
- (29) Lee, C.; Yang, W.; Parr, R. G. *Phys. Rev. B* **1988**, *37*, 785.
- (30) Schot, A. P.; Radom, L. *J. Chem. Phys.* **1996**, *100*, 16502.
- (31) Ditchfield, R. *Mol. Phys.* **1974**, *27*, 789.
- (32) Wolinski, K.; Hinton, J. F.; Pulay, P. *J. Am. Chem. Soc.* **1990**, *112*, 8251.
- (33) Gauss, J. *J. Chem. Phys.* **1993**, *99*, 3629.
- (34) *Recent advances in density functional methods*; Chong, D. P., Casida, M. E., Eds.; World Scientific: Singapore, 1995; Part 1.
- (35) El-Masry, A. H.; Fahmy, H. H.; Ali Abdelwahed, S. H. *Molecules* **2000**, *5*, 1429.
- (36) Lautie, A.; Hervieu, J.; Belloc, J. *Spectrochim. Acta* **1983**, *39A*, 367.